# Soft x-ray magnetic scattering evidence for biquadratic coupling in Co/Cu multilayers

T. P. A. Hase, I. Pape, D. E. Read, and B. K. Tanner
*Department of Physics, University of Durham, South Road, Durham DH1 3LE, United Kingdom*

H. Dürr,* E. Dudzik, and G. van der Laan
*Daresbury Laboratory, Daresbury, Warrington WA4 4AD, United Kingdom*

C. H. Marrows and B. J. Hickey
*Department of Physics and Astronomy, University of Leeds, Leeds LS2 9JT, United Kingdom*
(Received 28 July 1999; revised manuscript received 15 November 1999)

Soft x-ray resonant magnetic scattering has been used to study the magnetic structure of sputtered Co/Cu multilayers. A pure magnetic peak, at half the scattering vector of the structural Bragg peak from the multilayer, was observed from layers with and without deliberate oxygen contamination in the middle of the copper spacer layer. With increasing field in the sample plane, the magnetic peak intensity varied very differently for the two types of sample due to the high sensitivity of the magnetic scattering to changes in moment rotation in the sample plane. The data provide strong support for a model of biquadratic coupling in the contaminated samples and bilinear, antiferromagnetic coupling in the clean samples.

## I. INTRODUCTION

Despite being the subject of great attention, Co/Cu multilayers continue to provide new scientific twists to the understanding of the mechanism of giant magnetoresistance (GMR). It is well established that residual gases in sputtering chambers can have a significant effect on the properties of such multilayers, $H_2O$ and $O_2$ being particularly damaging.[1,2] However, more recently it has been suggested that a very low level of $O_2$ can be beneficial to the operation of spin valve structures.[3] In studies of the effect of residual gases at different positions in the multilayer,[4] Marrows *et al.* have found that, in contrast to equivalent clean samples, which exhibit high GMR and strong antiferromagnetic (AF) coupling with near zero remanence at 9 Å Cu spacer thickness, samples that were gas damaged in the middle of the spacer layers showed a reduction in GMR by a factor of 2, and a substantial remanent magnetization. By modeling magnetization, determined by the magneto-optic Kerr effect (MOKE) and GMR, Marrows and Hickey proposed that the interlayer coupling contains both bilinear and biquadratic components.[5] In the case of the gas-damaged samples, the biquadratic coupling dominates and the moments of adjacent Co layers are thus predicted to orient at close to right angles with each other. The moments of adjacent Co layers in the clean samples are expected to couple antiferromagnetically, as the bilinear term dominates. In order to provide additional support for this interpretation, we have undertaken soft x-ray resonant magnetic scattering experiments at the Co $L_3$ edge in varying magnetic fields. By studying, as a function of magnetic field, the intensity of the pure magnetic peak arising from antiferromagnetically coupled bilayers, we show that the coupling is very different and totally consistent with a biquadratic coupling model. We have also undertaken high- and low-angle scattering measurements with x rays tuned to the copper *K* absorption edge (8.98 keV) in order to characterize the interface structure and crystallographic texture of the samples.

Soft x-ray resonant magnetic scattering measurements at the $L_{2,3}$ edges of transition metals have recently been undertaken by a number of researchers. Kao *et al.*[6] observed large resonances in the scattering from a 35 Å iron layer deposited on GaAs in the vicinity of the $L_{2,3}$ edges of iron. They extended the calculation of Hannon *et al.*[7] but found that no significant corrections to the model were required to fit the data taken at the $L_{2,3}$ edges of the $3d$ transition metals. Several authors have used circularly polarized light tuned to the Co $L_3$ absorption edge to study magnetic multilayers[8,9] and spin valve structures.[10] Tonnerre *et al.*[11] and Hashizume *et al.*[12] have studied multilayer structures of Ni/Ag and Gd/Fe, respectively. They have shown that for antiferromagnetically coupled bilayers, a pure magnetic Bragg peak is observed at a $q$ vector half that of the first charge scattering Bragg peak from the multilayer. We have studied the equivalent peak in Cu/Co multilayers, originally observed by Séve *et al.*[13] The field dependence of this pure magnetic peak, which is also revealed in polarized neutron scattering, has very recently been used by Borchers *et al.*[14] to determine the domain structure in weakly coupled Co/Cu multilayers.

## II. EXPERIMENTAL DETAILS

Soft x-ray magnetic scattering measurements were performed on a two-circle diffractometer in a high vacuum chamber on stations 1.1 and 5U1 of the Daresbury Synchrotron Radiation Source (SRS). A spherical grating monochromator focused and monochromated the beam to provide a flux ($\sim 10^{10}$ photons/sec per 100 mA) at the sample, covering the energy range between 200 and 1000 eV, with a resolution of approximately 500 meV. The polarization state of the incident x rays on station 1.1 was approximately 70% circularly polarized, while that on station 5U1 was almost 100% linearly polarized (the flux and energy resolution are

 

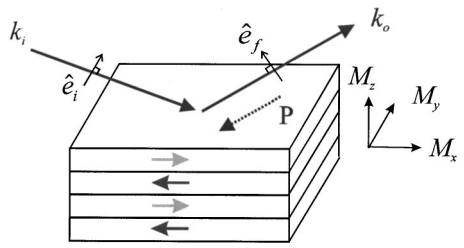


FIG. 1. Schematic diagram of the magnetic scattering geometry.

similar for both stations). The magnetic resonant scattering term is proportional to the vector product $(\hat{\mathbf{e}}_f \times \hat{\mathbf{e}}_i) \cdot \mathbf{M} = \mathbf{P} \cdot \mathbf{M}$ where $\hat{\mathbf{e}}_i$ and $\hat{\mathbf{e}}_f$ are unit vectors parallel to the incident and scattered beam polarization vectors, and $\mathbf{M}$ is the sample magnetization.[15] When the beam is linearly polarized in the horizontal plane and scattered into the vertical $(\sigma \rightarrow \pi)$, the experiment is sensitive only to the components of magnetization in the scattering plane beam (i.e., $M_x$ and $M_z$ in Fig. 1). Due to the anisotropy in these samples, the $M_z$ component of the magnetization is zero, and deviations away from this position can be thought of as magnetic roughness. The cross section for the magnetic $\sigma \rightarrow \sigma$ scattering is zero. The circularly polarized component of the incident beam introduces the possibility of $\pi \rightarrow \sigma$ as well as $\pi \rightarrow \pi$ scattering. The $\pi \rightarrow \sigma$ scattering is sensitive to the same components of magnetization as the $\sigma \rightarrow \pi$, but with a 180° phase shift. For an antiferromagnetically coupled sample, the $\pi \rightarrow \sigma$ and the $\sigma \rightarrow \pi$ scattering will result in a magnetic Bragg peak at half the $q$ vector of the structural Bragg peak. The cross product of the incident and exit polarizations for the $\pi \rightarrow \pi$ scattering lies perpendicular to the scattering plane, along the direction $M_y$. In the present experiments the magnetization component $M_y$ has the same sense for all cobalt layers. Any contribution to the magnetic scatter from the $\pi \rightarrow \pi$ scattering occurs solely at the structural Bragg peak position and not at the pure antiferromagnetic peak arising from the $M_x$ components. Comparison between data taken on stations 5U1 and 1.1 confirms that the $\pi$ component of polarization does not significantly influence the shape of the reflectivity profile.

Structural measurements were performed on station 2.3 of the Daresbury SRS at energies close to the $K$ absorption edge of Cu (8.98 keV). Grazing incidence specular and diffuse scattering provided data on the thickness of the multilayers and the interface structure, while scattering measurements around the 111 reciprocal lattice point provided data on grain size and crystallographic texture. Details of the experimental arrangement and measurement procedures can be found elsewhere.[16]

The results presented in this paper were obtained from a series of $[\mathrm{Cu}\ (9\ \text{Å})/\mathrm{Co}\ (10\ \text{Å})]_{50}$ multilayers deposited on Si(001) by magnetron sputtering. The base pressure of the system was $\sim 1\times10^{-7}$ Torr and growth of the samples was halted during the deposition of the copper spacer layer. Sample 1 acts as a control sample and the sample contains no gas contamination. The growth of the spacer layer in sample 2 was halted for 1 sec, while that for sample 3 was 10 sec. A delay of 10 sec results in a contamination level of approximately 0.1 Langmuir.

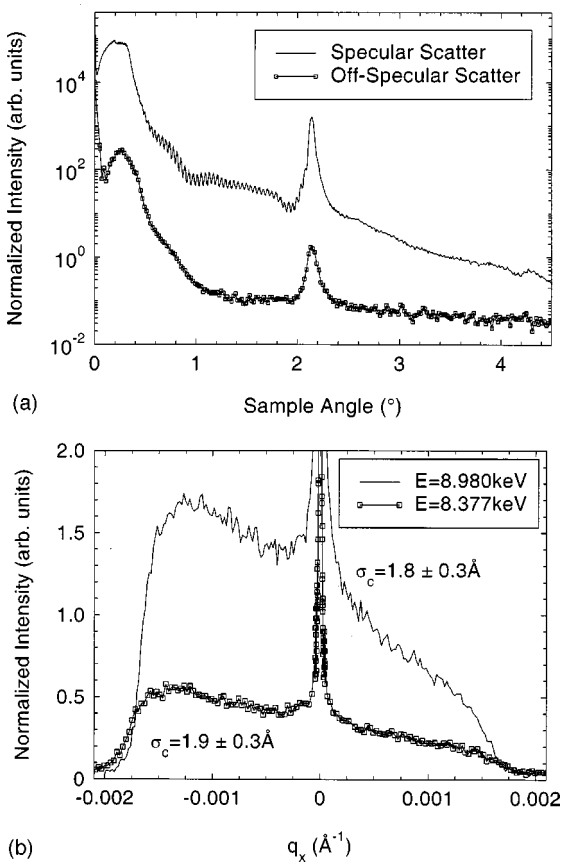


FIG. 2. Specular and off-specular scans at $E = 8.980$ keV (a) and transverse diffuse scans through the Bragg peak at and away from the Cu absorption edge (b) for sample 2.

## III. STRUCTURAL RESULTS

All samples gave remarkably similar grazing incidence x-ray scattering results, typified in Fig. 2 where we present the data from sample 2. From the Bragg peak position we find the bilayer thickness to be $18.5 \pm 0.3$ Å, and we can be certain that the magnetic and magnetotransport differences between the samples do not arise from differences in coupling strength due to different spacer layer thicknesses. All samples have extremely smooth interfaces with a well-defined Bragg peak being observed in the off-specular radial scans in reciprocal space. This indicates that the roughness in the samples is highly correlated, but the lack of Kiessig fringes in the off-specular scans implies that the correlation length normal to the surface is less than the multilayer thickness. Tuning the x-ray energy close to the Cu absorption edge causes a large change in the diffuse scatter measured in a transverse scan in reciprocal space though the Bragg peak. Away from the Bragg peak, the change is small, confirming that correlated roughness dominates. Born wave analysis of the diffuse scatter through the Bragg peak yields values of the correlated roughness varying between 1.2 and 1.9 $(\pm 0.3)$ Å for the various samples.

Around the 111 reciprocal lattice point, the scattering from the multilayer was difficult to detect, even for the zero-order peak. With Soller slits in front of the detector and a beam height of 1 mm the peak maxima were found to be approximately 100 counts per second. This geometry gave a resolution of better than $1.34\times10^{-4}$ Å$^{-1}$ in $q_z$ and 8.3

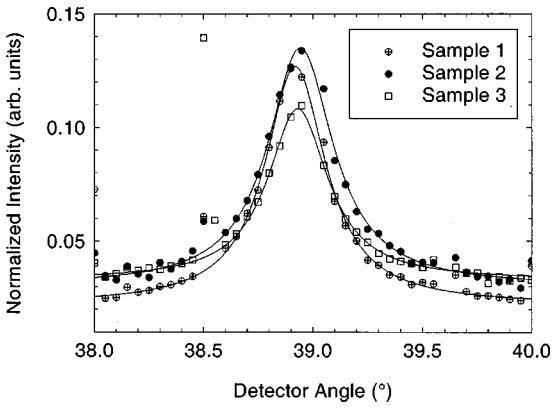


FIG. 3. $\theta/2\theta$ scans for the three samples in the vicinity of the Cu/Co 111 zero-order peak. $E=8.98$ keV. The isolated points arise from stray reflections from the (001) silicon substrate.

$\times 10^{-5}$ Å in $q_x$ (0.015° in angle for the rocking curves). In longitudinal scans, the zero-order Cu/Co 111 peak could be fitted satisfactorily to a Lorentzian (Fig. 3), and using the Scherrer equation we deduced a grain size of between 217 and 236 ($\pm 4$) Å for all samples. Again, no systematic trends could be found around the average value of 220 Å.

Transverse scans were also taken through the zero-order Cu/Co multilayer 111 peak. The peaks were well fitted by Gaussian functions (Fig. 4), the full width at half height maximum varying between 14.7° and 17.0°($\pm 0.5°$). The samples exhibit substantially less 111 texture than other sputtered Cu/Co multilayers that we have studied. Ion beam etching studies of substrates have shown that the GMR falls as the 111 texture improves, provided that the interface roughness remains constant.[17] The present poor texture, together with the small interface roughness, may account for the high GMR observed in these samples. However, the hard x-ray scattering results clearly show that there is no significant structural difference between the clean and gas-contaminated samples. Nuclear magnetic resonance[4] and high-resolution cross-sectional transmission electron microscopy[18] studies on similarly damaged samples also fail to reveal any differences in interface structure.

## IV. MAGNETIC SCATTERING MEASUREMENTS

Specular reflectivity profiles recorded as a function of x-ray energy (Fig. 5) show that tuning the x-ray energy into the Co $L_3$ edge results in a dramatic resonant enhancement of the magnetic scatter. A pure magnetic Bragg reflection from the antiferromagnetic coupled multilayers appears at a $q$ value which is half of that of the structural multilayer Bragg peak. The double $d$ spacing of the magnetic structure implies that the magnetic moment is coupled antiferromagnetically, but we cannot distinguish between bilinear and biquadratic coupling from this curve alone. (Magnetometry results suggest that this particular sample is biquadratically coupled.) No magnetic Bragg peak is observed when the energy is tuned to the Cu $L_3$ edge (Fig. 6), showing that there is no significant magnetic moment penetrating into the copper spacer layer.

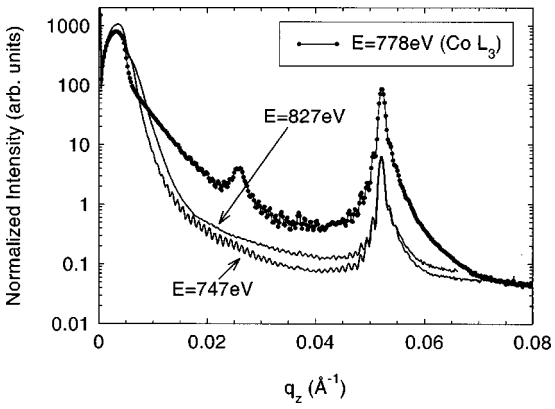


FIG. 5. Specular scans as a function of x-ray energy for sample 3 recorded on beamline 1.1, Daresbury SRS (70% circularly polarized).

As a function of x-ray energy, away from the resonance condition, all the reflectivity scans show a similar behavior (Fig. 5), although the scan taken at an energy of 827 eV shows weaker Kiessig fringes. When the energy is tuned to either the cobalt or copper $L_3$ edge, there is an enhancement of the specular scatter for all scattering vectors. The rate of fall of intensity with wave vector for the two energies is very similar (Fig. 6), with only the intensity of the Kiessig fringes differing at the two energies. We thus conclude that the intensity changes in the reflectivity observed in Fig. 5 are due to anomalous dispersion in the charge scattering rather than magnetic moment gradient or roughness.

Although the penetration depth in Fe/Co at the peak of the

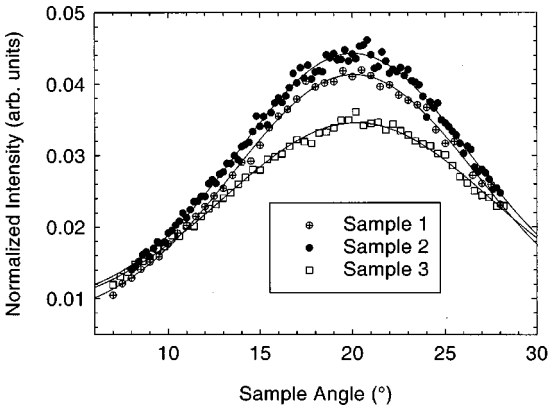


FIG. 4. Transverse diffuse (rocking curve) scans through the zero-order Cu/Co multilayer 111 peak. Experimental data (points) and Gaussian fits (lines).

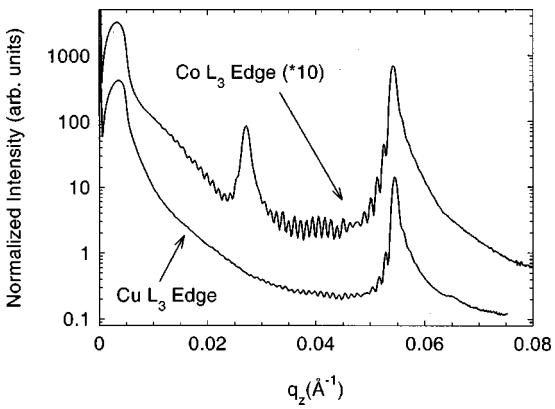


FIG. 6. Specular scans recorded from sample 1 at the Co (top line) and Cu (bottom line) $L_3$ resonances. The Co data have been offset by a factor of 10 for clarity.

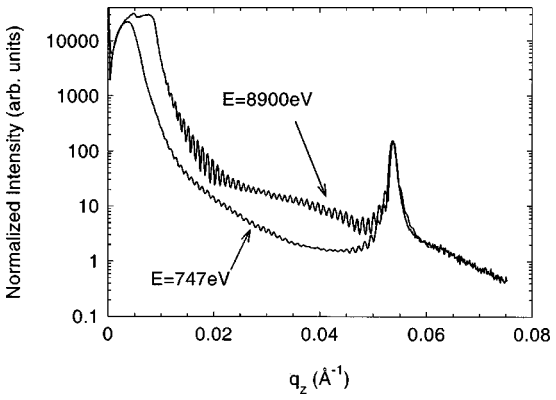


FIG. 7. Comparison of the specular reflectivity using hard (top line) and soft (bottom line) x rays as a function of wave vector $q_z$ normal to the plane for sample 2. The intensity has been normalized to the structural Bragg peak.

iron $L_3$ edge was found by Sacchi *et al.* to be less than 275 Å,[19] Fig. 7 shows that this is clearly not the case when slightly off resonance. Indeed, it was observed experimentally that the greatest magnetic signal occurred at energies just below the tabulated Co $L_3$ edge. At these energies, the absorption of the radiation was significantly lower than at resonance, and Kiessig fringes were also observed. Specular scans at 8.9 keV and 747 eV exhibit Kiessig fringes of the same period in wave vector $q_z$, corresponding to the total stack thickness. Thus, x rays at both wavelengths penetrate the approximately 1000 Å thick sample although at 747 eV the absorption is high and the fringe amplitude is correspondingly low. The large absorption of the soft x rays also results in a blurring of the critical angle.

The field dependence of the pure magnetic peak was investigated initially by applying a 730 Oe field parallel to the beam direction, using an external, permanent magnet and subsequently measuring the specular scatter in zero field. A field of approximately 500 Oe was then applied orthogonal to the beam using an *in situ* electromagnet, and the specular scatter again recorded in zero field. Figure 8 shows the intensity of the magnetic peak that was recorded after the application of the two fields for the bilinear samples. The only effect of changing the magnetization direction is in the intensity of the magnetic peak. An increase in the magnetic peak intensity is observed when the field is applied perpendicular to the x-ray beam. These data are considerably clearer than the work on Cu/Co multilayers previously published by Séve *et al.*[13] In their paper, the magnetic scattering was weak and obscured by the Kiessig fringes.

The biquadratically coupled sample 3 showed a magnetic peak at the same momentum transfer as the bilinearly coupled sample. However, the dependence of this magnetic peak on the applied magnetic field direction was very different from the other, bilinear samples. Figure 9 shows the specular scans across the magnetic peak for the two orthogonal magnetization directions. There was no observed change in the intensity of the magnetic peak with applied field in this sample. Thus, the configuration of the spins in the biquadratic samples must remain the same for both applied field directions.

The intensity of the magnetic peak was measured as a function of applied field perpendicular to the beam. The

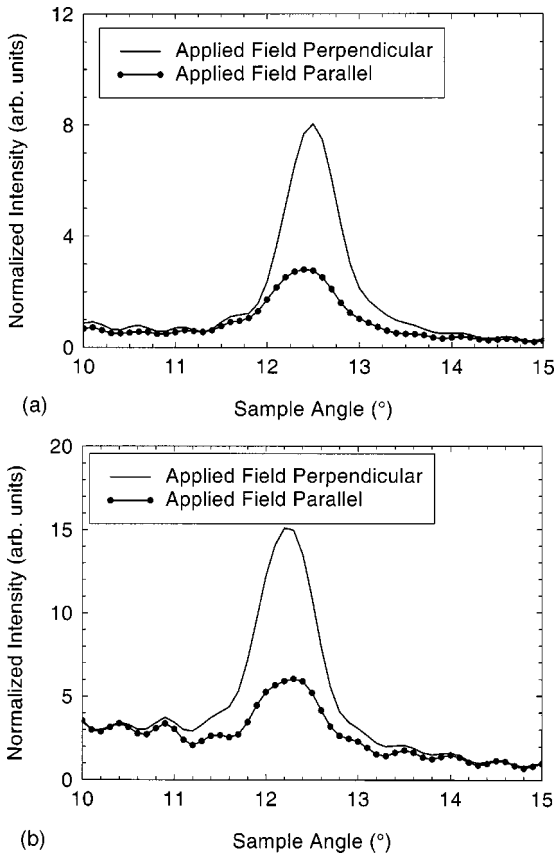


FIG. 8. Remanence specular magnetic Bragg peak after applied field in the scattering plane for the bilinear samples: sample 1 (a) and sample 2 (b). Line, field applied perpendicular to the beam, and points with the field parallel to the beam direction.

samples were initially subjected to a field of 730 Oe applied along the beam direction as before, and the intensity of the magnetic peak was recorded after a field had been applied for 5 sec transverse to the beam direction. A further measurement was taken after the field had been removed. A new, higher field was then applied and the sequence continued. Figure 10 shows the variation of the magnetic peak intensity as a function of field applied in this manner for sample 2 (bilinear). Both bilinear samples exhibited similar behavior.

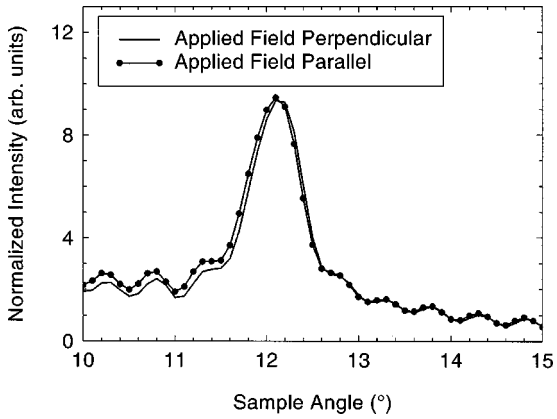


FIG. 9. The magnetic peak intensity with the field applied along (points) and perpendicular to (line) the beam for the biquadratic sample.

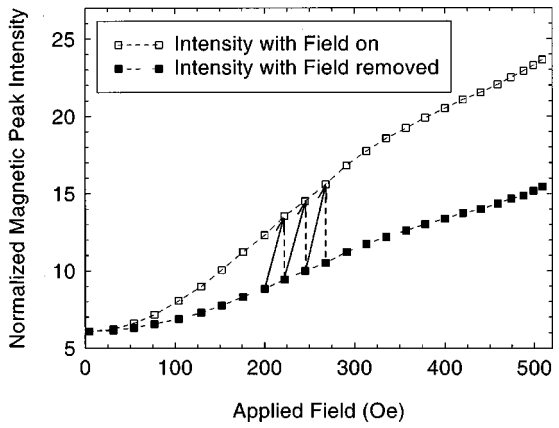


FIG. 10. Magnetic peak intensity as a function of applied field for sample 2. Data recorded in a rising sequence (arrows) with the field alternately on (open points) and off (closed points).

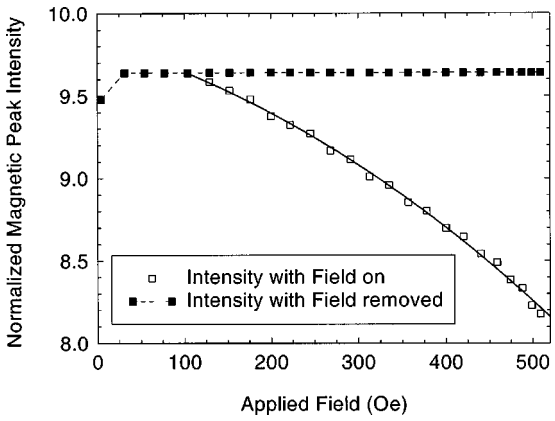


FIG. 12. Magnetic peak intensity as a function of sequentially applied field for sample 3. Data recorded with the field on (open points) and off (closed points).

Little change in the magnetic peak intensity is observed for fields below 100 Oe. Thereafter, a steady increase in the intensity both with and without field is observed. No saturation was observed in the magnetic peak intensity, even for an applied field in excess of 500 Oe. After the orthogonal field had been thus applied, the magnetic peak intensity in zero field had increased by a factor of almost 3, in agreement with Fig. 8(b).

The intensity change between zero field and a previously applied field is reversible (Fig. 11). Here the sample had been magnetized perpendicular to the beam by applying and removing the field up to a maximum of 510 Oe as in Fig. 10. From the last closed data point in Fig. 10, we then applied and removed the field sequentially along the previously magnetized direction. The intensity of the magnetic peak increases steadily as the orthogonal field step is increased (Fig. 11) but the magnetic peak intensity in zero field does not change significantly. On removal of the field, the magnetic peak intensity fell sharply, with a subsequent slow decay to the initial value being observed over a period of minutes.

The experiment equivalent to that of Fig. 10 was undertaken on the biquadratically coupled sample. It showed a very different behavior from that of the bilinear samples (Fig. 12). Beyond 100 Oe, the with-field magnetic peak intensity falls on the application of an orthogonal field, there being no increase in the zero-field value through the sequence. In this region, where the peak intensity follows a parabolic dependence on the applied field strength, the changes are reversible. A slight increase in the peak intensity on application of a field was observed for low fields.

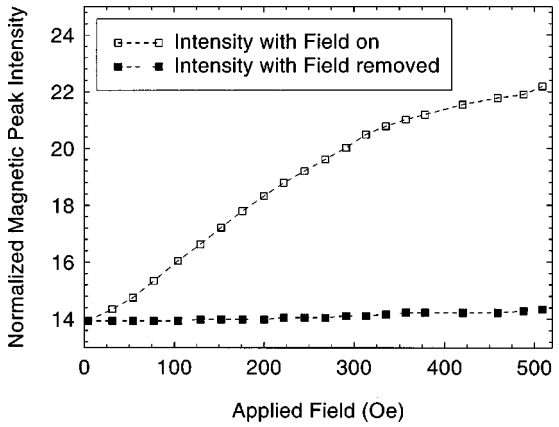


FIG. 11. The field dependence on further sequential application and removal of a field, starting at the last closed data point in Fig. 10.

## V. DISCUSSION

Soft x-ray magnetic scattering experiments can be modeled by assuming that the coupled moments are rotating in the sample plane. In the deposition chamber a small field of approximately 100 Oe is used to align the magnetic layers, and this defines an easy axis of magnetization. In the current experiments the *in situ* orthogonal field was applied along this direction, i.e., in the plane of the sample and perpendicular to the beam direction. When the spins couple biquadratically, a large net moment associated with the coupling is present, Fig. 13(a). This is confirmed by Lorentz electron microscopy on similar samples.[20] In the virgin state, the net moment aligns parallel or antiparallel to the easy direction.

On application of a weak external field, the moments rotate to align the net ferromagnetic component parallel to it, and form a single-domain state. The layers always remain coupled due to the strong exchange coupling inherent in these systems. When the orthogonal field is still further increased, the angle between the spins in adjacent layers is

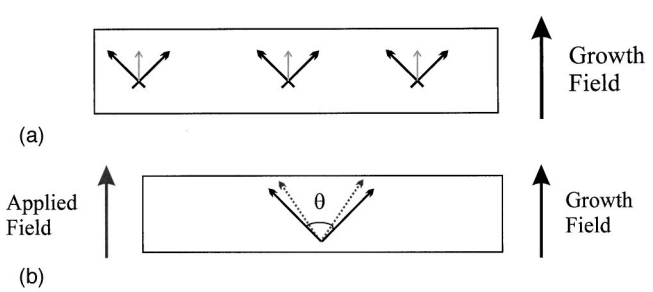


FIG. 13. (a) The as-grown magnetic state of the biquadratic sample. (b) The biquadratic sample on the application of a large field along the easy axis.

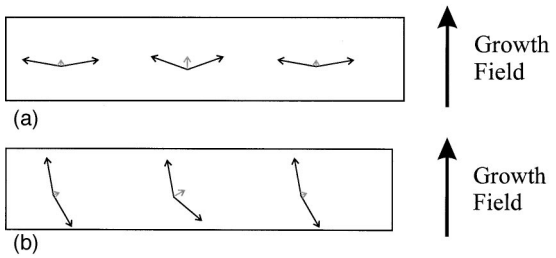


FIG. 14. (a) The as-grown magnetic state of the bilinear samples. (b) The magnetic structure of the bilinear samples, on removal of the external field applied along the beam direction.

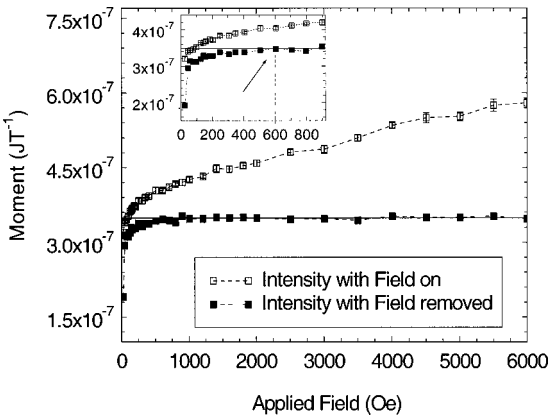


FIG. 15. Magnetization versus field measured in the growth field direction. The field was applied in a rising sequence of steps, reverting to zero between each step, as in Fig. 10. Below 600 Oe the zero-field magnetization rises with applied field as in the soft x-ray scattering data.

reduced [Fig. 13(b)]. This reduction in angle corresponds to a reduction in the component of magnetization parallel (along) the beam, and therefore a reduction in the magnetic peak intensity is observed (cf. Fig. 11). When the field is removed, the individual layer moments reversibly rotate back away from the easy axis, opening the angle again and increasing the magnetic peak intensity.

In a purely bilinear, antiferromagnetically coupled sample, there should be almost no magnetic peak intensity when the sample is magnetized along the beam direction. There was a substantial magnetic peak still visible, however, implying either that the sample contained biquadratic domains, or that the antiferromagnetic alignment was not perfect. Lorentz microscopy[20] indicates that the latter case occurs, leaving a small moment which aligns with the growth field. The as-grown state, therefore, has the layer moments lying almost along the beam direction, with the small moment associated with the coupling pointing along the growth field direction [Fig. 14(a)].

The Lorentz microscopy results suggest, however, that the anisotropy field is low and that the difference in energy between the two orthogonal directions is very small. As in the biquadratic sample, the moments rotate toward an external field applied along the beam direction. However, unlike in the biquadratic sample, the net moment will not necessarily rotate back to the easy axis on removal of the external field, being pinned in local energy minima at intermediate directions [Fig. 14(b)]. The large magnetic ripple that is seen in the Lorentz micrographs confirms this interpretation.[20]

When an orthogonal field is applied, the net moment starts to rotate back toward the easy direction. This motion is determined by the free-energy surface, and it requires relatively large fields to rotate the net moment back toward the easy axis. Such changes are consistent with the variations seen in Fig. 10. The change of the magnetic peak intensity is proportional to the projection of the layer moment along the beam direction. Our results indicate that the maximum angle of rotation of the moment was approximately 60°. When the field is removed, some of the moments rotate away from the global minimum corresponding to the easy axis toward a local energy minimum. This results in a reduction in the magnetic peak intensity. Figure 11 maps out reversible changes about a particular energy minimum. If it were possible to apply a large field, the intensity of the magnetic peak in the bilinear samples should saturate and then start to reduce in intensity for the same reasons as the biquadratic sample.

The irreversible changes observed in Fig. 10 do not relate directly to the low-field hysteresis seen in MOKE measurements or its associated domain wall motion observed in Lorentz microscopy. In our samples, the coercive field is approximately 20 Oe and no domain wall motion is seen above this value.[20] The hysteresis seen in the soft x-ray scattering data is associated with rotational processes not normally studied. In magnetization curves taken under equivalent geometrical conditions on a vibrating sample magnetometer, very similar behavior was observed (Fig. 15). Again, the AF coupled sample (number 1) was first saturated perpendicular to the growth field direction, after which the field was sequentially increased and reduced to zero along the growth field direction. We note significant hysteresis below 600 Oe (inset) where the magnetization in zero field does not return to a single value, consistent with rotation of the moments and only partial relaxation on removal of the field. Beyond about 600 Oe, the zero-field magnetization remains constant and the steady increase of the in-field magnetization corresponds to reversal closure of the AF coupled moments toward the field direction.

## VI. CONCLUSION

Soft x-ray resonant magnetic scattering experiments, which have measured the intensity of a pure magnetic Bragg peak as a function of applied field in two orthogonal directions, have been used to study the effects of gas contamination in the spacer layer on the coupling within Co/Cu multilayers. The data show that uncontaminated samples are antiferromagnetically coupled and the field dependence is consistent with a small canting of the moments in adjacent cobalt layers. This results in a complex anisotropy energy surface that displays substantial hysteresis. High-sensitivity magnetometry measurements also show evidence of hysteresis when the in-plane rotation of the net moment is measured in a similar configuration.

Gas-contaminated samples show a radically different behavior on application of fields parallel to the growth field direction. In contrast to samples coupled antiferromagneti-

cally, the intensity of the pure magnetic Bragg peak, which still appears at a $q$ value corresponding to twice the chemical repeat distance, falls with increasing field. A quadratic dependence of the with field intensity and the absence of hysteresis can only be interpreted in terms of orthogonal coupling of the cobalt layers. This alignment, which has a period of twice the cobalt/copper multilayer spacing, arises from dominance of the biquadratic term in the exchange coupling between cobalt layers. In zero field, the net moment lies along the growth field direction. Our results provide powerful support for the coupling model containing both bilinear and biquadratic terms invoked to explain the magnetotransport and magnetization data.[5]

## ACKNOWLEDGMENTS

The authors would like to thank the staff at the Daresbury SRS who provided the diffractometer and station facilities during the taking of the data, in particular, Ian Kirkman and Mark Roper. Funding from EPSRC is acknowledged. C. H. Marrows thanks the Royal Commission for the Exhibition of 1851 for financial support.

*Present address: Institut für Festkörperforschung, Forschungszentrum Jülich, 52425 Jülich, Germany

[1] F. Yoshizaki and T. Kingetsu, Thin Solid Films **239**, 229 (1994).
[2] K. Kagawa, H. Kano, A. Okabe, A. Suzuki, and K. Hayashi, J. Appl. Phys. **75**, 6540 (1994).
[3] W.F. Egelhoff, P.J. Chen, C.J. Powell, M.D. Stiles, R.D. McMichael, J.H. Judy, K. Takanoand, and A.E. Berkowitz, J. Appl. Phys. **82**, 6142 (1997).
[4] C.H. Marrows, B.J. Hickey, M. Malinowska, and C. Mény, IEEE Trans. Magn. **33**, 3675 (1997).
[5] C.H. Marrows and B.J. Hickey, Phys. Rev. B **59**, 463 (1999).
[6] C. Kao, J.B. Hastings, E.D. Johnson, D.P. Siddons, G.C. Smith, and G.A. Prinz, Phys. Rev. Lett. **65**, 373 (1990).
[7] J.P. Hannon, G.T. Trammell, M. Blume, and D. Gibbs, Phys. Rev. Lett. **61**, 1245 (1988); **62**, 2644(E) (1989).
[8] C.-C. Kao, C.T. Chen, E.D. Johnson, J.B. Hastings, H.J. Lin, G.H. Ho, G. Megis, J.-M. Brot, S.L. Hulbert, Y.U. Idzerda, and C. Vettier, Phys. Rev. B **50**, 9599 (1994).
[9] V. Chakarian, Y.U. Idzerda, C.-C. Kao, and C.T. Chen, J. Magn. Magn. Mater. **165**, 52 (1997).
[10] J.W. Freeland, V. Chakarian, Y.U. Idzerda, S. Doherty, J.G. Zhu, J.-H. Park, and C.-C. Kao, Appl. Phys. Lett. **71**, 276 (1997).
[11] J.M. Tonnerre, L. Séve, D. Raoux, G. Soullié, and B. Rodmacq, Phys. Rev. Lett. **75**, 740 (1995).
[12] H. Hashizume, N. Ishimatsu, O. Sakata, T. Iizuka, N. Hosoito, K. Namikawa, T. Iwazumi, G. Srajer, C.T. Venkataraman, J.C. Lang, C.S. Nelson, and L.E. Berman, Physica B **248**, 133 (1998).
[13] L. Séve, J.M. Tonnerre, D. Raoux, J.F. Bobo, M. Piecuch, M. De Santis, P. Troussel, J.M. Brot, V. Chakarian, C.C. Kao, and C.T. Chen, J. Magn. Magn. Mater. **148**, 68 (1995).
[14] J.A. Borchers, J.A. Dura, J. Unguris, D. Tulchinsky, M.H. Kelly, C.F. Majkrzak, S.Y. Hsu, R. Loloee, W.P. Pratt, Jr., and J. Bass, Phys. Rev. Lett. **82**, 2796 (1999).
[15] J.P. Hill and D.F. McMorrow, Acta Crystallogr., Sect. A: Found. Crystallogr. **A52**, 236 (1996).
[16] T.P.A. Hase, I. Pape, B.K. Tanner, and M. Wormington, Physica B **253**, 278 (1998).
[17] D.E. Joyce, C.A. Faunce, P.J. Grundy, B.D. Fulthorpe, T.P.A. Hase, I. Pape, and B.K. Tanner, Phys. Rev. B **58**, 5594 (1998).
[18] M. Ormston, A.K. Petford-Long, C.H. Marrows, and B.J. Hickey (unpublished).
[19] M. Sacchi, C.F. Hague, E.M. Gullikson, and J.H. Underwood, Phys. Rev. B **57**, 108 (1998).
[20] C.H. Marrows, B.J. Hickey, M. Herrmann, S. McVitie, J.N. Chapman, M. Ormston, A.K. Petford-Long, T.P.A. Hase, and B.K. Tanner, Phys. Rev. B **61**, 4131 (2000).